Geol. Mag. **144** (*2*), *2007, pp. 379–392.* © *2007 Cambridge University Press*

doi:10.1017/S0016756806003074 First published online 9 February 2007 *Printed in the United Kingdom*

Late Miocene transcurrent tectonics in NW Turkey: evidence from palaeomagnetism and ^{40}Ar–^{39}Ar dating of alkaline volcanic rocks

N. KAYMAKCI*, E. ALDANMAZ†, C. LANGEREIS‡, T. L. SPELL§, O. F. GURER† & K. A. ZANETTI§

*RS/GIS lab. Department of Geological Engineering, Middle East Technical University, Ankara 06531, Turkey
†Department of Geology, University of Kocaeli, Izmit 41040, Turkey
‡Faculty of Earth Sciences, Utrecht University, Budapestlaan 17, 3584 CD Utrecht, The Netherlands
§Isotope Geochronology Laboratories, Dept. of Geosciences, University of Nevada, Las Vegas, NV 89154–4110, USA

(*Received* 10 August 2005; *accepted* 5 June 2006)

Abstract – A number of intra-continental alkaline volcanic sequences in NW Turkey were emplaced along localized extensional gaps within dextral strike-slip fault zones prior to the initiation of the North Anatolian Fault Zone. This study presents new palaeomagnetic and ^{40}Ar–^{39}Ar geochronological results from the lava flows of NW Turkey as a contribution towards understanding the Neogene–Quaternary tectonic evolution of the region and possible roles of block rotations in the kinematic history of the region. ^{40}Ar–^{39}Ar analyses of basalt groundmass indicate that the major volume of alkaline lavas of NW Turkey spans about 4 million years of episodic volcanic activity. Palaeomagnetic results reveal clockwise rotations as high as 73° in Thrace and 33° anticlockwise rotations in the Biga Peninsula. Movement of some of the faults delimiting the areas of lava flows and the timing of volcanic eruptions are both older than the initiation age of the North Anatolian Fault Zone, implying that the region experienced transcurrent tectonics during Late Miocene to Pliocene times and that some of the presently active faults in the region are reactivated pre-existing structures.

Keywords: palaeomagnetism, block rotation, ^{40}Ar–^{39}Ar ages, alkaline volcanism, NW Turkey, strike-slip faulting, North Anatolian Fault Zone.

1. Introduction

The Neogene tectonic evolution of NW Turkey has been largely influenced by the development of a number of strike-slip fault systems that resulted from collision of the African and Arabian plates with the Eurasian Plate. The main collision between the Eurasian and Arabian plates took place along the Bitlis–Zagros Suture Zone (Fig. 1a) and is also assumed to have caused the major shortening and uplift in Eastern Anatolia and the westward extrusion of the Anatolian Block (Mckenzie, 1972; Şengör, Görür & Şaroğlu, 1985). Internal deformation within the Anatolian Block as a result of this collision involved both internal imbrication and the formation of numerous strike-slip faults and related structures. The development of the latter may have been influenced by lateral variations of lithospheric rheology and the pre-existing structural framework (Dewey *et al.* 1986). The westward escape of the Anatolian Block is coupled with back-arc extension in the Aegean and accommodated by two major strike-slip faults: the dextral North Anatolian Fault Zone and the sinistral East Anatolian Fault Zone. Interaction of the westwards motion of the Anatolian Block with the dextral strike-slip motion of the North Anatolian Fault Zone and roughly N–S-directed Aegean extension system (Gürer *et al.* 2003; Flerit *et al.* 2004) led to a change in the movement of the Anatolian Block relative to the Eurasian Plate from westwards to southwestwards as the style of deformation also changed from pure strike-slip along the eastern to transtensional mechanisms along the western segments of the North Anatolian Fault Zone. These relationships also led to anticlockwise rotation of the Anatolian Block (Rotstein, 1984; Oral *et al.* 1995; Reilinger *et al.* 1997; McClusky *et al.* 2000) and bifurcation of the North Anatolian Fault Zone into a number of dextral strike-slip faults with normal components and development of small distributed pull-apart basins in NW Turkey (Fig. 1b).

The Neogene tectonic evolution of the Thrace basin is less well understood but has been attributed to the Thrace Fault Zone (e.g. Perinçek, 1991; Turgut, Türkaslan & Perinçek, 1991; Görür & Okay, 1996). According to Perinçek (1991), the Thrace fault is the abandoned westernmost extension of the North Anatolian Fault Zone and has not played a significant role in the tectonic development of the region since the Late Miocene. More recently, Yaltırak & Alpar (2002) proposed that many of the strike-slip faults in NW Turkey (including the Edremit, Yenice, Etili, and Ganos faults; Fig. 1) are dextral splay faults of the 'so called' Thrace–Eskişehir Fault Zone and played a major role in tectonic development of the region prior to

*Author for correspondence: kaymakci@metu.edu.tr

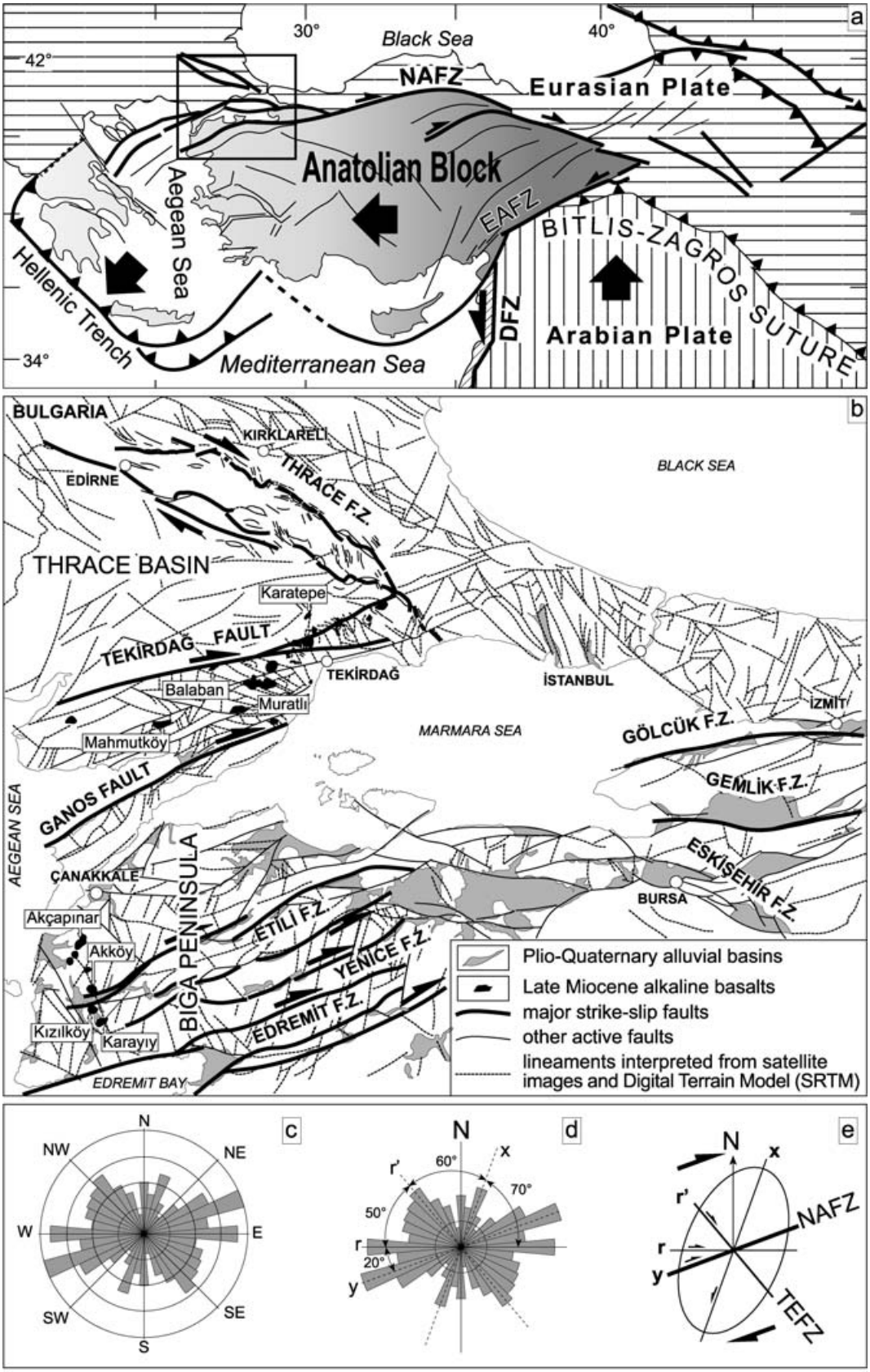

Figure 1. (a) Map showing the major tectonic elements and plate reconstruction of eastern Mediterranean. DFZ – Dead Sea Fault Zone, EAFZ – East Anatolian Fault Zone, NAFZ – North Anatolian Fault Zone (compiled from Şengör, Görür & Şaroğlu, 1985; Barka, 1992; Barka & Hancock, 1984; Kaymakci, White & van Dijk, 2003; Bozkurt, 2001; Gürer *et al.* 2003). Large arrows indicate plate motion directions; triangles indicate active convergent zones (ticks are on the upper plate). (b) Map of NW Turkey showing the structural elements (in addition to our observations and Remote Sensing studies, compiled from Perinçek, 1991; Siyako, Bürkan

the development of the North Anatolian Fault Zone in Quaternary times. In contrast, Zattin, Okay & Cavazza (2005) proposed that the North Anatolian Fault Zone has been active since the Late Oligocene. Although the origin of the strike-slip faults in the region is still debatable, both studies indicate that a number of dextral strike-slip faults were active in the region during the emplacement of the basaltic lavas in the Late Miocene.

Here, we shed some light on the tectonic development of NW Turkey by integrating the results of palaeomagnetic measurements and radiometric dating of basaltic lavas, and we note possible relationships between regional tectonic activity and the development of mantle-derived mafic alkaline lavas during the Late Miocene.

2. Structures

The major structures in NW Turkey are mainly dextral strike-slip fault systems, including various branches of the North Anatolian Fault Zone and the Thrace and Eskişehir fault zones (Sakınç, Yaltırak & Oktay, 1999). In addition, a number of lineaments, which have not been reported previously, are recognizable from Landsat ETM+ and ASTER imagery and Shuttle Radar Topography Mission (SRTM) elevation data obtained from the USGS (Fig. 1). Among these lineaments, the Tekirdağ Fault is one of the most striking structures in the region. This fault extends from the southwest corner of the Thrace basin to the southeast end of the Thrace Fault Zone. Using the deflected streams and morphological features the Tekirdağ Fault is interpreted as a dextral strike-slip fault zone with no recent activity. The fault delimits the northern boundary of the alkaline basalt outcrops in the north and is sub-parallel to the strike of the recently active Ganos Fault. The alkaline basalt outcrops in the Thrace Basin are delimited in the south by the Ganos Fault, which also controls the western boundary of the Sea of Marmara and the Gulf of Saros (Fig. 1b). A number of recent investigations have examined the nature, evolution and deformation mechanism of the Ganos Fault along with its earthquake potential (Tüysüz, Barka & Yiğitbaş, 1998; Okay *et al*. 2000; Okay, Tüysüz & Kaya, 2004; Sato *et al.* 2004).

The Biga Peninsula (Fig. 1b) is traversed from northeast to southwest by a number of strike-slip faults (including the Edremit, Yenice and Etili fault zones) which result in a zone of distributed deformation in NW Turkey. Focal mechanism solutions of the earthquakes on some of these fault zones indicate that they have been recently active and have dextral strike-slip motions (Eyidoğan, 1988).

The other, less pronounced but widely distributed, structures are generally confined to the blocks delimited by NE-trending major faults. The lengths of these structures range from a few kilometres to a few tens of kilometres. They further divide the NE-trending fault blocks defined and delimited by the major structures into relatively equidimensional smaller (few tens of kilometres long and wide) fault blocks which may be subjected to rotational deformation (this is discussed later). The rose diagram prepared from all the structures including the interpreted lineaments indicates that most of the structures are developed in four pronounced directions (Fig. 1c), averaging 250° N, 270° N, 320° N and 020° N. Other directions are less pronounced. The striking feature of the rose diagram is that the Thrace and Eskişehir fault zones can be interpreted as the antithetic Riedel shears (r') of the North Anatolian Fault Zone. This implies that they must be sinistral fault zones, although it is unequivocally accepted that (Perinçek, 1991; Turgut, Türkaslan & Perinçek, 1991; Okay *et al*. 2000; Yaltırak & Alpar, 2002) these faults were dextral strike-slip fault zones and they cannot be the antithetic Riedel shears of the North Anatolian Fault Zone. This further implies that parallel orientation of antithetic Riedel Shears (r') and the Thrace and Eskisehir fault zones is just coincidental. Therefore, their activity was terminated since their dextral nature is incompatible with the new tectonic regime which gave way to the development of the North Anatolian Fault Zone in post-Late Miocene times.

3. Nature of the volcanic activity

The alkaline basaltic lava flows in the region are exposed in two linear belts in the Thrace and in the Biga Peninsula separated from each other by the northernmost segment of the North Anatolian Fault Zone (Ganos Fault: Yaltırak & Alpar, 2002). In the Biga Peninsula, the volcanic field is aligned N–S and comprises a number of sub-horizontal lava flows lying in localized extensional basins formed by strike-slip movements related to activity along the Edremit, Yenice and Etili faults (Fig. 1b). The lavas have an irregular base and show development of soil horizons. Lava moraines are observed between the individual flows, and well-developed columnar jointing is observed near the eruptive centres. The lavas in this area are mainly fine-grained olivine-phyric or aphyric basalts and basanites that are suggested to have originated from decompression melting of sub-lithospheric (asthenospheric) mantle sources (e.g. Aldanmaz, 2002; Aldanmaz *et al.* 2000).

& Okay, 1992; Yaltırak, 1996, 2002; Yılmaz & Polat, 1998; Yılmaz & Karacık, 2001, Yaltırak & Alpar, 2002), distribution of the mafic alkaline volcanic products (modified from Ercan *et al.* 1995), actively developing basins, and locations of palaeomagnetic and geochronological sampling sites (text in boxes). (c) Rose diagram prepared from the trends of the structures indicated in the map. (d, e) Interpretation of frequency of the structures according to simple shear Riedel pattern proposed by Dresen (1992).

Table 1. Summary of ^{40}Ar–^{39}Ar results

Locality	Material used	Preferred age (Ma)	Total fusion age	Weighted mean plateau age	Inverse isochron age	K–Ar age*
Thrace						
Karatepe	WR	11.68 ± 0.25	11.23 ± 0.13	–	11.68 ± 0.25	–
Balaban	WR	8.43 ± 0.07	8.43 ± 0.07	–	–	–
Muratlı	WR	8.62 ± 0.36	8.95 ± 0.18	8.62 ± 0.36	–	–
Mahmutkoy	WR	8.53 ± 0.35	8.94 ± 0.32	8.53 ± 0.35	–	–
Biga Peninsula						
Akçapınar	WR	11.16 ± 0.21	11.50 ± 0.21	11.16 ± 0.21	–	11.30 ± 0.40
Akkoy (Ezine)	WR	8.08 ± 0.14	8.08 ± 0.14	–	–	9.70 ± 0.33
Kızılköy	WR	9.97 ± 0.14	9.97 ± 0.14	–	–	10.01 ± 0.20
Karayıy	WR	7.65 ± 0.36	9.30 ± 0.35	7.65 ± 0.36	–	8.32 ± 0.19

WR – groundmass concentrates from whole-rock samples; all uncertainties are 2 SD (95% confidence level) in Ma.
*Compiled from Paton (S. M. Paton, unpub. Ph.D. thesis, Cambridge Univ., London, 1992); Ercan *et al.* (1995); Aldanmaz *et al.* (2000).

In the Thrace volcanic field, the alkaline volcanic activity formed a number of isolated lava flows with a maximum thickness of 100 m (Fig. 1). The alkaline volcanic field lies to the southern margin of the Thrace basin as the eruption centres are linearly distributed along the margin and aligned approximately in a NW–SE direction within a zone delimited by the Tekirdağ Fault in the north and Ganos Fault in the south. The lavas that erupted along NNW-trending strike-slip faults form the southernmost border of the triangle-shaped Thrace basin (Fig. 1). The alkaline volcanic rocks from the Thrace volcanic field are compositionally identical to those from the Biga Peninsula and are interpreted to have originated from the same source (e.g. Yılmaz & Polat, 1998; Aldanmaz *et al.* 2006; Aldanmaz, Gourgaud & Kaymakci, 2005).

4. The ^{40}Ar–^{39}Ar geochronology

4.a. Analytical techniques

A total of nine samples were collected, from the sites analysed palaeomagnetically, for age determinations by the ^{40}Ar–^{39}Ar incremental heating method. The analyses were performed in the Nevada Isotope Geochronology Laboratory at the University of Nevada, Las Vegas. Samples were selected based on their freshness, degree of crystallinity (e.g. abundances of phenocrysts and glass), and the level of uncertainty in their existing age assignment. All samples used in this study are alkaline basalts or basanites and lack a suitable high-K phenocryst phase. For glass-free basaltic lavas, however, reliable results can be obtained by ^{40}Ar–^{39}Ar incremental heating of groundmass concentrates (e.g. Gans, 1997). Care was taken to sample fresh rocks from the more slowly cooled interiors of lava flows likely to possess a glass-free groundmass.

Splits of original core samples (not subject to demagnetization) were first carefully examined petrographically to determine which were sufficiently fresh and had the least amount of glass in the groundmass. Those deemed suitable for dating were lightly crushed and sieved to varying size fractions (100–200 μm to 300–500 μm, depending on the sample) and ultrasonically cleaned in deionized water. Standard magnetic separation techniques and handpicking were used to generate groundmass concentrates. Irradiated samples were analysed using conventional furnace step heating in a double vacuum resistance furnace similar to the Staudacher *et al.* (1978) design (see also Spell & McDougall, 2003 for procedures). Analyses ranged from 8 to 13 step heating experiments for each sample, focusing on the gas released between 600 and 1000 °C, as this component of the gas generally has the highest radiogenic yields and is considered the most reliable (e.g. Mankinen & Dalrymple, 1972). Details of nine new age determinations are summarized in Table 1 with selected age spectra and inverse isochron plots illustrated in Figure 2.

4.b. Results of the ^{40}Ar–^{39}Ar analyses

Incremental heating spectra yielded apparent age plateaus defined as comprising three or more contiguous steps corresponding to at least 50 % of the total ^{39}Ar released and showing no significant slope, with the individual step ages agreeing within 2σ errors with the weighted mean age of the plateau segment. Most of the samples analysed yielded well-behaved ^{40}Ar–^{39}Ar data with easily interpretable ages and uncertainties. Some of the samples yielded fairly 'flat' age spectra having well-defined plateaus or pseudo-plateaus (Fig. 2), indicating that the samples are undisturbed and have been closed systems since initial crystallization. Individual spectra for some other samples, however, range from hump-shaped to U-shaped to L-shaped, a range of spectral characteristics that is typical of fresh basaltic rock suites (e.g. Gans, 1997) and is readily explainable in terms of the combined effects, but variable contributions, of reactor-induced recoil, low temperature argon loss, and a non-atmospheric 'trapped' component (that is, excess argon; ^{40}Ar–$^{36}Ar > 295.5$) (e.g. Mankinen & Dalrymple, 1972). Some of the samples gave total fusion ages (the age that would have been obtained had the sample been run in a single step) substantially older than the weighted

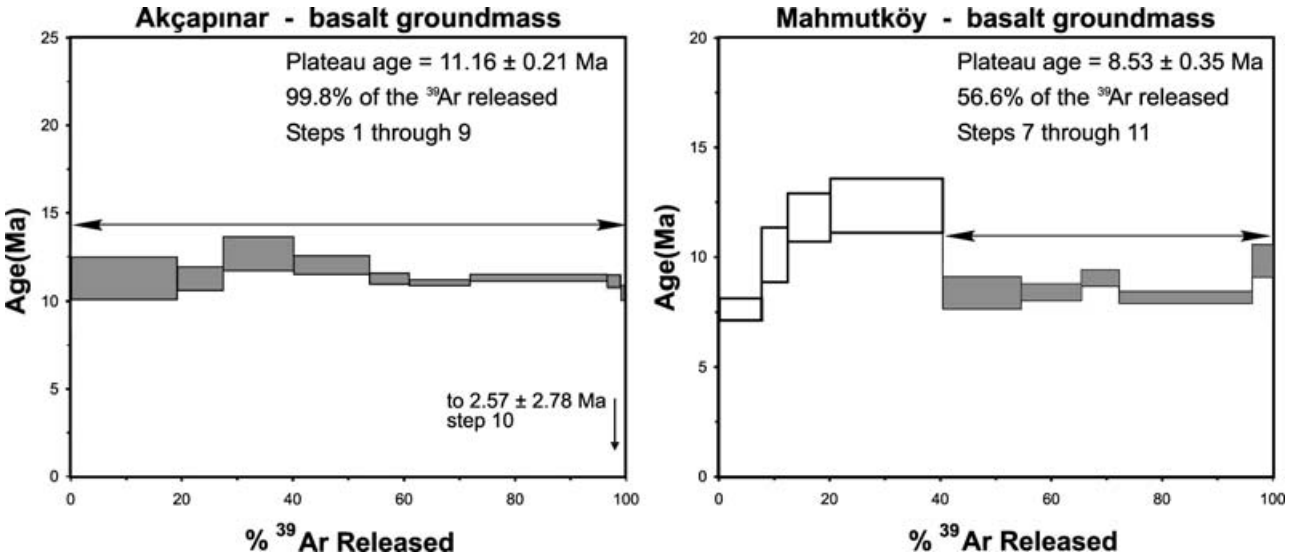

Figure 2. ^{40}Ar–^{39}Ar age spectra for selected palaeomagnetic samples from the alkaline volcanic suite of NW Turkey. All data from incremental heating experiments are plotted as apparent age of each temperature step versus the cumulative fraction of ^{39}Ar gas released. Steps used in the weighted mean plateau age calculations are shaded black. Inset window for each sample depicts the inverse isochron plot with the calculated isochron age and $^{40}Ar/^{39}Ar$ ratio of the trapped component for the same data. Temperatures for each step are in °C. All errors (illustrated by each step thickness on the spectra and by the size of the boxes on the isochron plots) are estimated 1SD errors without the error in J (flux parameter).

Table 2. Results from natural remanent magnetization (NRM) analysis from the sites in northwest Anatolia

Site	Age	N	D (°)	I (°)	k	α	Rot. (°) and sense	Temp. range (°C)
Thrace								
Balaban	8.43 ± 0.07	7	243.8	− 58.4	75.9	7.7	64 c	330–630
Karatepe	11.68 ± 0.25	6	32.8	66.2	211.4	4.6	33 c	430–630
Mahmutköy A	8.53 ± 0.35	6	237	− 76	283.7	4	57 c	180–480
Mahmutköy B	8.53 ± 0.35	7	253	− 62.4	94.1	6.3	73 c	150–580
Muratli	8.62 ± 0.36	7	342.8	57.2	876.9	2	17 a	280–630
Biga Peninsula								
Akçapınar	11.16 ± 0.21	7	22.1	62.8	771.4	2.2	22 c	230–580
Akköy	8.08 ± 0.14	7	353.3	55.3	445.1	2.9	6.7 a	150–430
Karayıy	7.65 ± 0.36	5	342.3	10.9	24.5	15.8	17 a	100–230
Kızılköy	9.97 ± 0.14	5	147.3	− 54.1	168.4	5.9	33 a	150–530

N – number of specimens; D, I – site mean ChRM declination and inclination; k – Fisher's precision parameter; α – 95% cone of confidence; Rot. – magnitude of rotation; c – clockwise, a – anticlockwise rotation with a 0 reference direction.

mean plateau age, on account of the older apparent ages associated with the high temperature steps. The total fusion age is analogous to what would have been obtained in a conventional K–Ar age, and this discrepancy may explain why in some samples, the ages obtained by the ^{40}Ar–^{39}Ar method were slightly younger than the published K–Ar ages (see Table 1).

Groundmass concentrates were analysed for all samples of holocrystalline lavas. Typical confidence estimates range from 70 to 350 ka for 7 to 11 Ma samples. All samples with a known stratigraphical context yielded ages in the correct order, thus strengthening our confidence in the reliability of their age determinations. Basalts collected from the Thrace volcanic field yielded ages of 8.43 ± 0.07 to 11.68 ± 0.25 Ma, indicating a substantially longer period of volcanic activity than estimated by the previous ^{40}Ar–^{39}Ar and K–Ar data (e.g. 6–7 Ma: S. M. Paton, unpub. Ph.D. thesis, Cambridge Univ., London, 1992; Ercan *et al.* 1995). Samples from the Biga Peninsula also yielded ages of 7.65 ± 0.36 to 11.16 ± 0.21 Ma, a range similar to that of the Thrace lavas. Overall, the geochronological data indicate that the major volume of mafic alkaline lavas in NW Turkey spans about 4 million years of episodic volcanic activity, making the site an ideal place to investigate the local and regional tectonic rotations during and after this period.

5. Palaeomagnetism

5.a. Procedures and rock magnetic analyses

A total of 63 drill cores were taken from nine sites in the alkaline volcanic suite of NW Turkey (Fig. 1; Table 2), except for the Mahmutköy B site, where samples were collected from an approximately 1 m diameter block of medium-bedded sandstone and mudstone alternation contained within and baked by the lava flows. All other sites were individual lava flows chosen because

of their accessibility and structural coherence. Within each flow, at least seven drill-core samples were taken per site using a water-cooled gas-powered portable rock drill. In addition to these, large blocks of oriented hand samples were also collected as backups from each site. Samples were oriented using a magnetic compass, and magnetic directions were checked by back-sighting using a Brunton compass.

In the laboratory, each core sample was cut to standard sample sizes for measurement. The spare parts of each core sample together with the oriented hand samples are stored in the laboratory.

Specimens were measured at Utrecht University, Forthofddijk Laboratories (Netherlands). The natural remanent magnetization (NRM) was measured on a 2G Enterprises DC SQUID horizontal cryogenic magnetometer. Demagnetizations were made using thermal demagnetization techniques with a laboratory-built furnace. At least seven specimens per site were analysed using progressive stepwise thermal demagnetization at temperature ranges of 20°, 50°, 100°, 150°, 180°, 230°, 280°, 330°, 380°, 430°, 480°, 530°, 580° and 630°. Since all the lava flows were subhorizontal, no tectonic/tilt correction was applied to the measurements.

5.b. Palaeomagnetic results

The detailed palaeomagnetic results and corresponding ^{40}Ar–^{39}Ar ages age listed in Table 2. Vector component diagrams (Zijderveld, 1967) through selected data points were used to determine the NRM components (Fig. 3). When the results show a linear decay, usually towards the origin, a magnetization vector is determined. The magnetization vectors were averaged using Fisher (1953) statistics to calculate mean directions per site (Fig. 3, Table 2), from which tectonically induced rotations could be determined. As it is still unclear to which stable region northwestern Turkey formerly belonged, the results are not compared to a pole of a known reference plate, but are instead compared to 0° as a reference direction. The present-day overprint is removed in the lower temperature levels except for the samples collected from the Balaban and Karatepe sites (Fig. 3a, b), where it is in the range of 330 °C to 430 °C. A secondary component is sometimes present (Fig. 3c) and is generally removed between 150 and 230 °C. It has a viscous remanence possibly caused by weathering, although extremely fresh samples were used. A characteristic remanent magnetization (ChRM) component is removed at higher temperatures and shows both normal and reversed polarities. Most sites reveal ChRM components which had unblocking temperatures of 580–630 °C (Fig. 3a–g) residing in magnetite (Table 2). Demagnetization at higher temperatures results in randomly directed components. These samples have a relatively high NRM intensity (6–13 mAm^{-1}). Some samples, which are demagnetized at temperatures around 230–430 °C (Fig. 3h, i) and have relatively low intensities (0.8 mAm^{-1}) have ChRM components. We show an example of a completely overprinted sample with a relatively high intensity (72 mAm^{-1}) and a signal largely destroyed around 230 °C (Fig. 3i).

In the Biga peninsula only one site (Fig. 4g) yielded clockwise rotation (21°) while all other sites yielded anticlockwise rotations between 7° and 33° (Table 2). In the Thrace field, on the other hand, four sites yielded clockwise rotations between 34° and 73°, and only one site (Fig. 4f) yielded anticlockwise rotation (17°). Except for the Karayıy site where very low palaeoinclination (11°) is obtained (Fig. 4i) and for the Mahmutköy A site where a very high (−76°) palaeoinclination is obtained, the palaeoinclinations in all other sites are relatively consistent and range between 54° and 66° (Table 2).

6. Discussion

6.a. Distribution of palaeomagnetic directions

It is noticeable that there is a very distinct pattern in the distribution of the palaeodeclination directions in Thrace and the Biga Peninsula (Fig. 5a). In Thrace, with one exception (the Muratlı site), all sites yielded very high clockwise rotations in the range of 33° to 73°, while in the Biga Peninsula anticlockwise rotations are dominant (except one site: the Akçapınar) and range from 7° to 33°. Similar clockwise and anticlockwise rotations obtained in the region by Tapırdamaz & Yaltırak (1997) and İşseven (T. İşseven, unpub. Ph.D. thesis, Technical Univ. İstanbul, 2001) are depicted in Figure 5b for comparison. The pattern of determined and compiled palaeodeclinations indicates that very high clockwise rotations are constrained within a well-defined area (Fig. 5b) between the Tekirdağ and Ganos faults. Other areas are characterized by either little clockwise (e.g. Karatepe) and/or anticlockwise rotations in accordance with the present anticlockwise rotation of the Anatolian Block (Reilinger *et al.* 1997; McClusky *et al.* 2000). In other words, large clockwise rotations (60° in average) are concentrated within the area delimited by the Tekirdağ and Ganos faults and the amount of clockwise rotation outside of this zone is around 30° on average.

A number of different models have been postulated for the block rotations along vertical axes within strike-slip fault zones. However, it is useful to consider simplified models, since strike-slip fault zones are complex due to changes in the fault trace and incompatibilities due to space problems between rotating blocks (Biddle & Christie-Blick, 1985; Sylvester, 1988; Twiss & Moores, 1992). According to Ron *et al.* (1984), the amount of rotation is related to the width of the rotating block, the initial angle between the faults and the boundary of the domain, and the amount

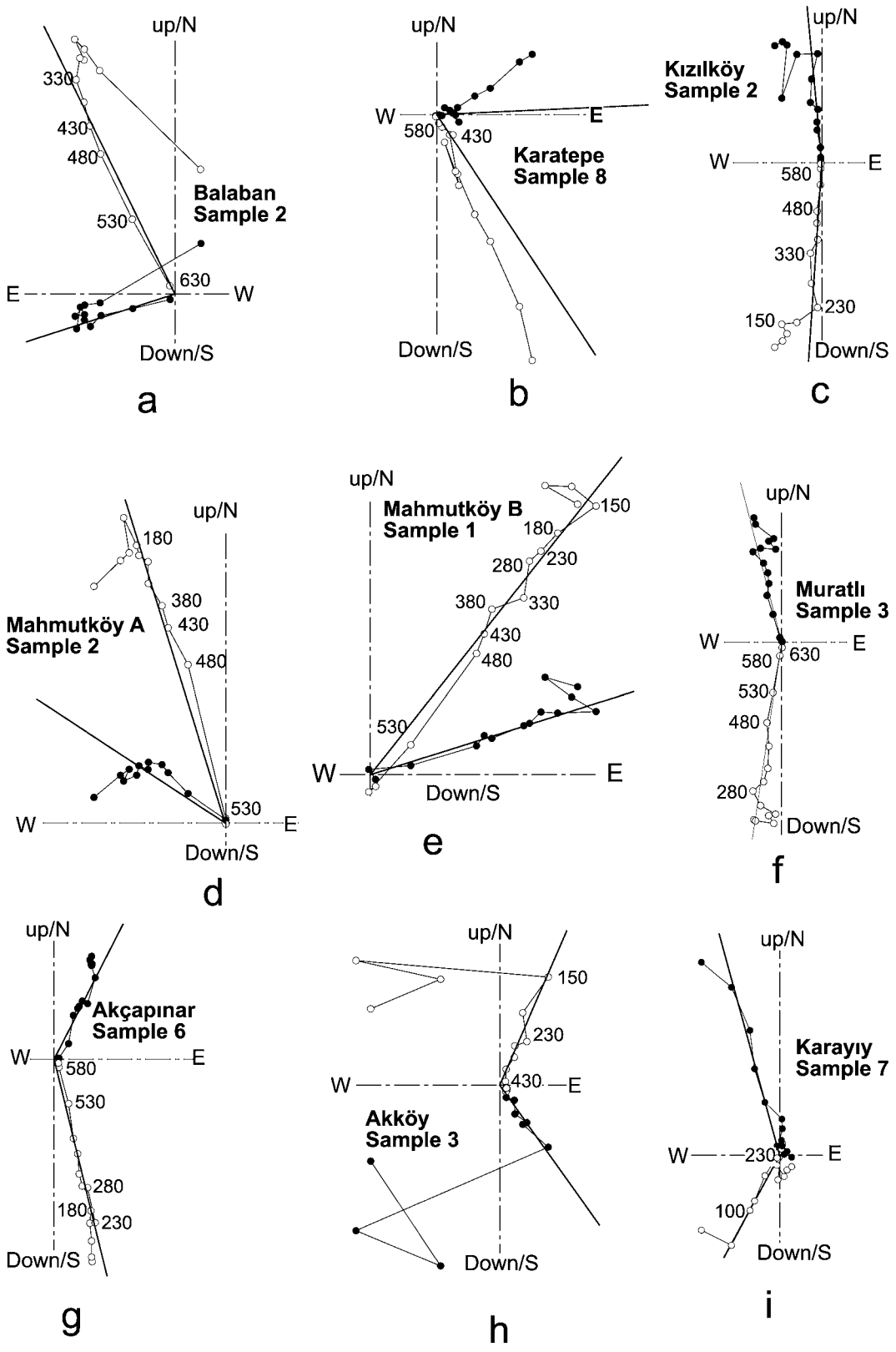

Figure 3. Orthogonal projections of stepwise thermal demagnetization of selected samples from each site. Closed (open) circles represent the projection of the ChRM vector endpoint on the horizontal (vertical) plane. Numbers adjacent to data points indicate ChRM interval temperatures (in °C).

of displacement (Fig. 6a). The model proposed by Garfunkel (1989) also predicts generalized rotations but in an opposite sense with respect to the main strike-slip displacement (Fig. 6b). Both models and their combination (Fig 6c, d) can be applied to the block rotations observed in NW Turkey.

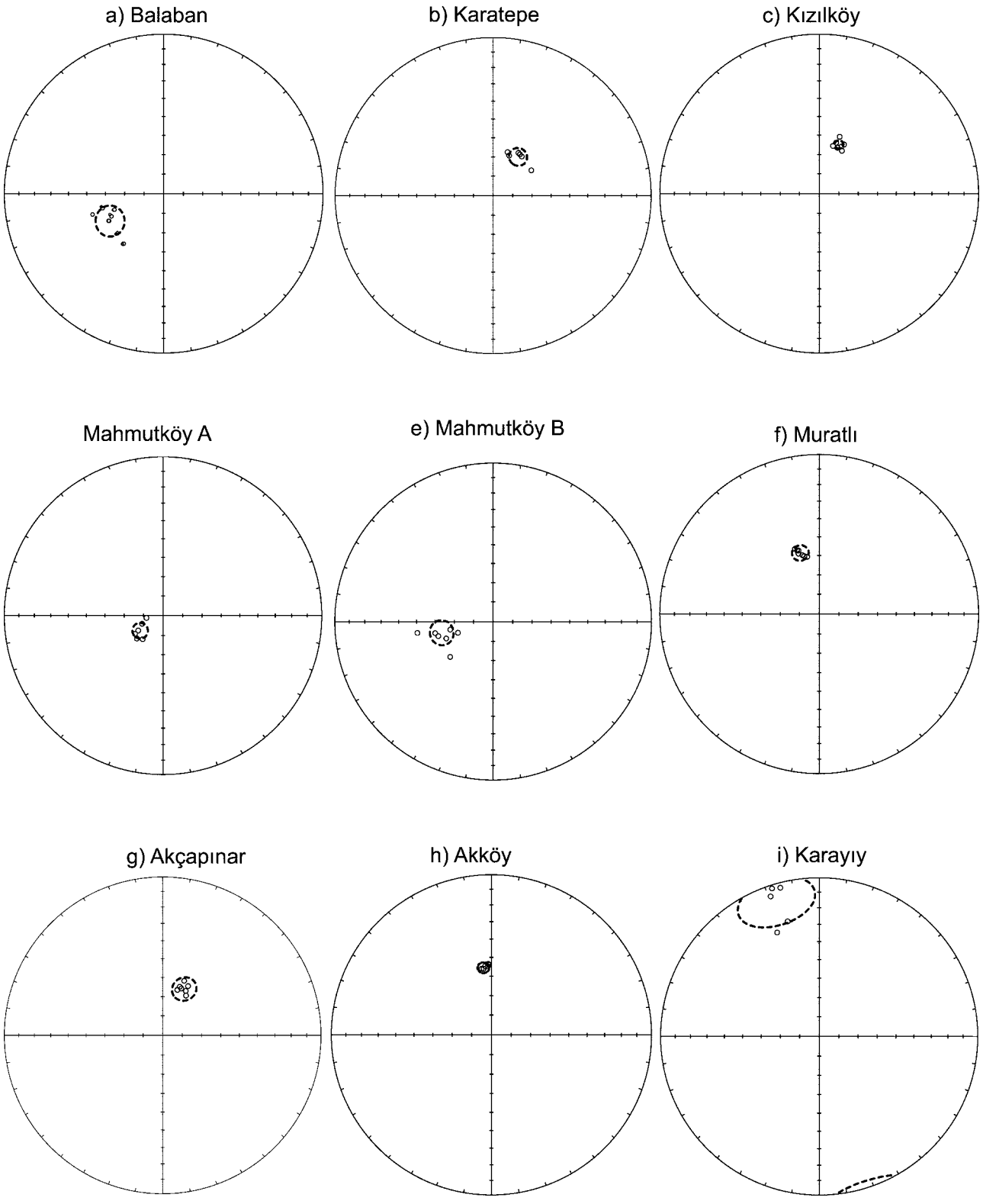

Figure 4. Equal area projection of all natural remanent magnetization (NRM) directions for all specimens. Dashed ellipses indicate $\alpha = 95$ % confidence intervals. Equal area, lower hemisphere projection.

The Tekirdağ Fault is, as discussed previously, thought to be a dextral strike-slip fault and was active prior to mid-Pliocene times. We infer that the area between the Tekirdağ and Ganos faults is divided into small blocks by a number of short faults (Fig. 5b). Due to dextral shearing of the area between the Tekirdağ and Ganos faults, we suggest that these blocks have rotated clockwise during the Late Miocene to the Early Pliocene interval when the Tekirdağ Fault was active. This gave way to the development of releasing

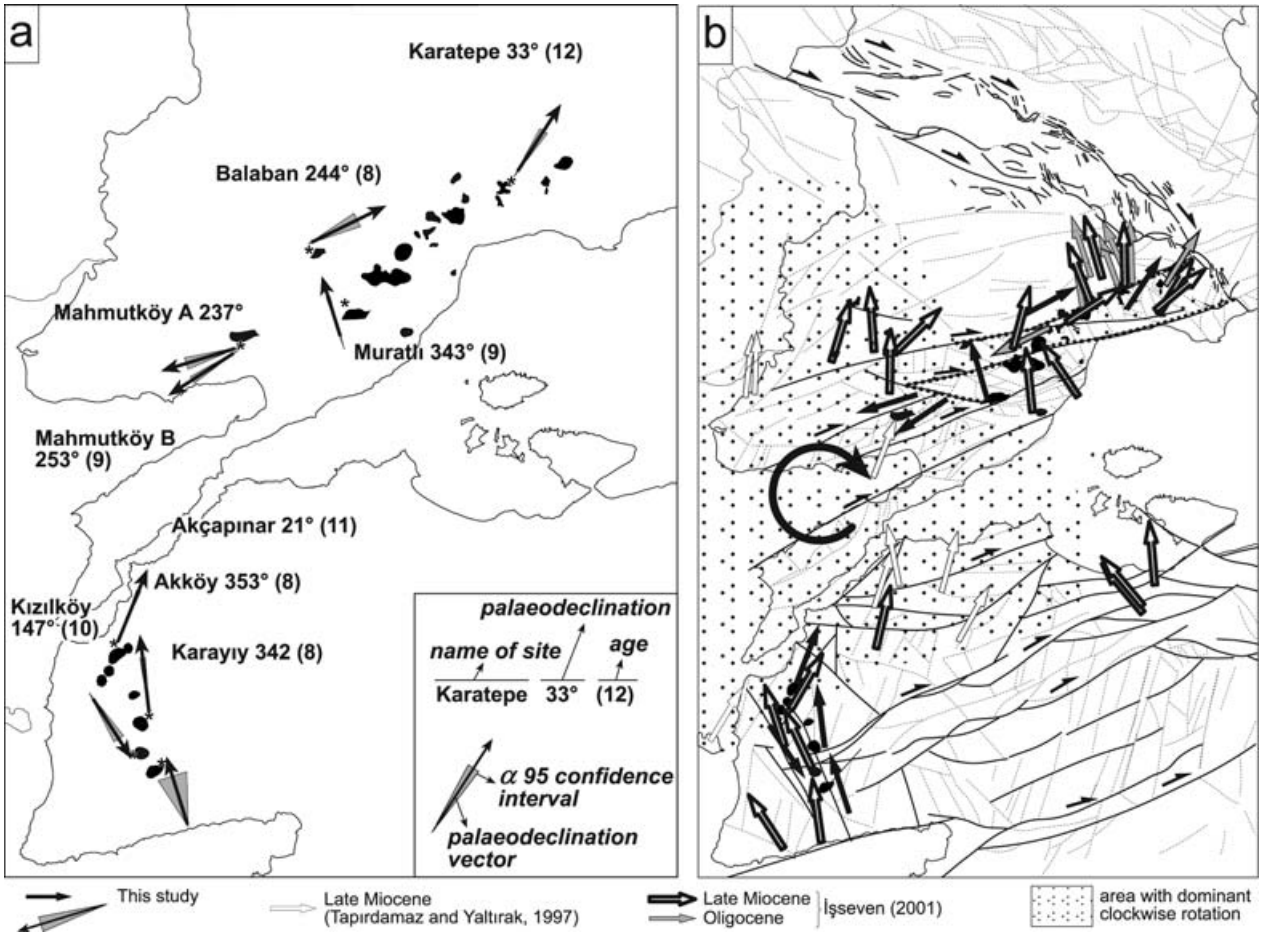

Figure 5. (a) Distribution of determined palaeodeclinations and basalt outcrops. (b) Structural map of NW Anatolia and compiled palaeodeclinations. The areas with clockwise rotation are indicated with stippled pattern. İşseven (2001) – T. İşseven, unpub. Ph.D. thesis, Technical Univ. İstanbul, 2001.

bends and/or releasing stepovers which in turn allowed eruption and rotation of the basaltic lavas. The amount of clockwise rotation of the blocks within the fault zone is at least 30°. As mentioned previously, the lava flows within this zone are rotated in a clockwise sense by up to 60°, which implies that the region underwent a further clockwise rotation of more than 30°. In other words, the combination of the local 30° and regional 30° clockwise rotations gave way to cumulative 60° (and higher) clockwise rotation of the blocks within the area between the Takirdağ and Ganos faults. Areas outside this zone have experienced only the regional rotations of 30° since the Late Miocene (Fig. 7).

6.b. Regional implications

Anticlockwise rotations in most areas of Turkey and especially the Anatolian Plate have already been recognized for post-Pliocene times using palaeomagnetic (Kissel & Laj, 1988; Platzman *et al.* 1994; Platzman, Tapırdamaz & Sanver, 1998; Tatar *et al.* 1995, 2004; Kaymakci *et al*. 2003; Kissel *et al.* 2003; Piper *et al.* 1996; Piper, Gürsoy & Tatar, 2002; Gürsoy *et al.* 1997; Gürsoy, Piper & Tatar, 2003; Duermeijer *et al.* 1999) and Global Positioning System (GPS) studies (Reilinger *et al.* 1997; McClusky *et al.* 2000; Kotzev *et al*. 2001; Provost, Chéry & Hassani, 2003). Therefore, anticlockwise rotations in the Biga Peninsula are attributed to the North Anatolian Fault Zone.

Two possible models can account for the origin of clockwise rotations in the region. In the first model, it is proposed that clockwise rotations are localized within the fault zones and that there is little or no regional rotation similar to the mechanism proposed by Ron *et al.* (1984) (see Fig. 6). This means that both the clockwise and anticlockwise rotations are due to distributed complex deformation of the region. Therefore, the 60° clockwise rotations in the area between the Tekirdağ and Ganos faults is due to dextral shearing of the zone. In that case, taking the width of the zone (D – distance between Ganos Fault and Tekirdağ Fault) as 30 km (Fig. 7a) and an average clockwise rotation (α) of 60° yields a minimum dextral movement (displacement, x) of 26 km ($x = 1/2D.\tan\alpha$). Twenty-six kilometres of dextral displacement is approximately equal to the cumulative offset values estimated for the North Anatolian Fault Zone (Barka & Hancock, 1984;

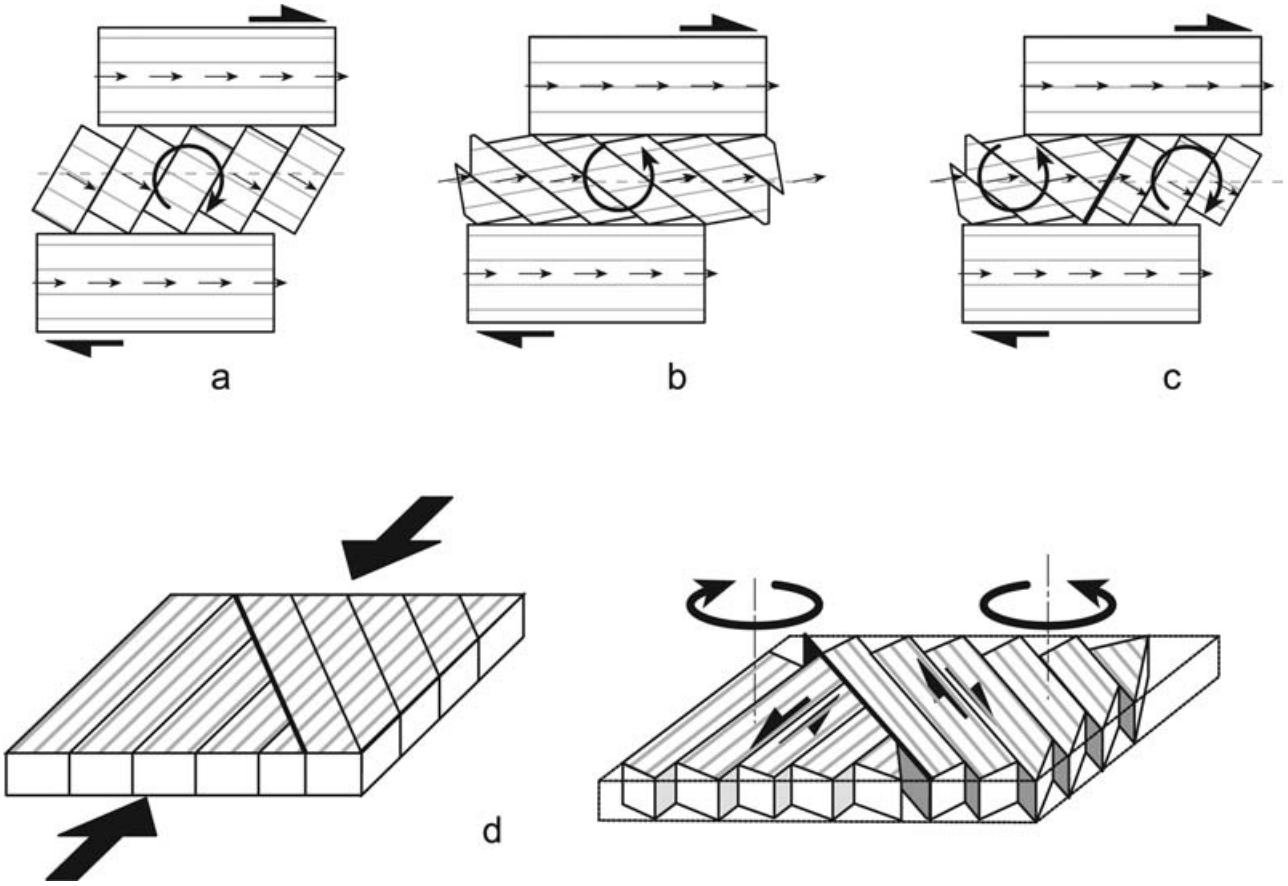

Figure 6. Various rotation models proposed by (a, c, d) Ron *et al.* (1984) and (b) Garfunkel (1989). Arrows on the blocks indicate palaeomagnetic vectors.

Şaroğlu, 1988; Koçyiğit, 1989) since Late Miocene times. This may imply that rotations in the Thrace basin are related to the North Anatolian Fault Zone and that the Tekirdağ Fault is also currently active. Our field studies and seismic data (Coşkun 1997, 2000; Turgut, Türkaslan & Perinçek, 1991) and recent GPS studies, however, indicate that the Tekirdağ Fault is no longer active and possibly deactivated prior to mid-Pliocene times. Therefore, we suggest that about 30° of the clockwise rotations relate to pre-mid-Pliocene movements of the Tekirdağ and Ganos faults, while the remaining 30° clockwise rotation is due to cumulative dextral regional rotation since the Late Miocene (Fig. 7). Thus, cumulative dextral offset should be corrected to 13 km allowing for 30° cumulative clockwise rotation within the zone.

Taking the second (latter) model into consideration, the region is restored tentatively (Fig. 7). After restoration (back-rotation) of the basalt outcrops according to determined average rotation amounts, all the basalt outcrops would have been oriented N–S and therefore collinear or even parallel to each other (Fig. 7b). Thus, all of the northern and southern outcrops may once have been aligned N–S so that basaltic eruption took place along a N–S-oriented fracture system extending from the Edremit Bay in the south to the Thrace Fault Zone in the north. Possibly they attained their present day configuration due to differential block rotations later imposed by the North Anatolian Fault Zone. This implies very large-scale deformation and clockwise rotations in NW Turkey which have not been reported previously. Similar clockwise rotations in the range of 20–30°, however, are reported in the north Aegean and in the Balkan region (Dimitriadis, Kondopoulou & Atzemoglou, 1998; Van Hinsbergen, 2004) and are also observed in the sites outside of the area between the Tekirdağ and Ganos faults. Therefore, it is most likely that local fault zone controlled rotations and regional rotations might have operated in the region and the observed rotations are the cumulative result.

The recent GPS studies, mentioned above, indicate that the Thrace Basin north of the Ganos Fault is relatively inactive to weakly active. Only the areas close to the Ganos Fault and the Tekirdağ Fault indicate southwesterly movement relative to Eurasia (Okay, Tüysüz & Kaya, 2004). It is generally accepted that these rotations are related to activity on the North Anatolian Fault Zone, implying that large-scale rotations in the region must have been acquired prior to mid-Pliocene and Quaternary activities in the region. This subsequently leads to a conclusion that some of the faults in the region, including the Ganos Fault, are

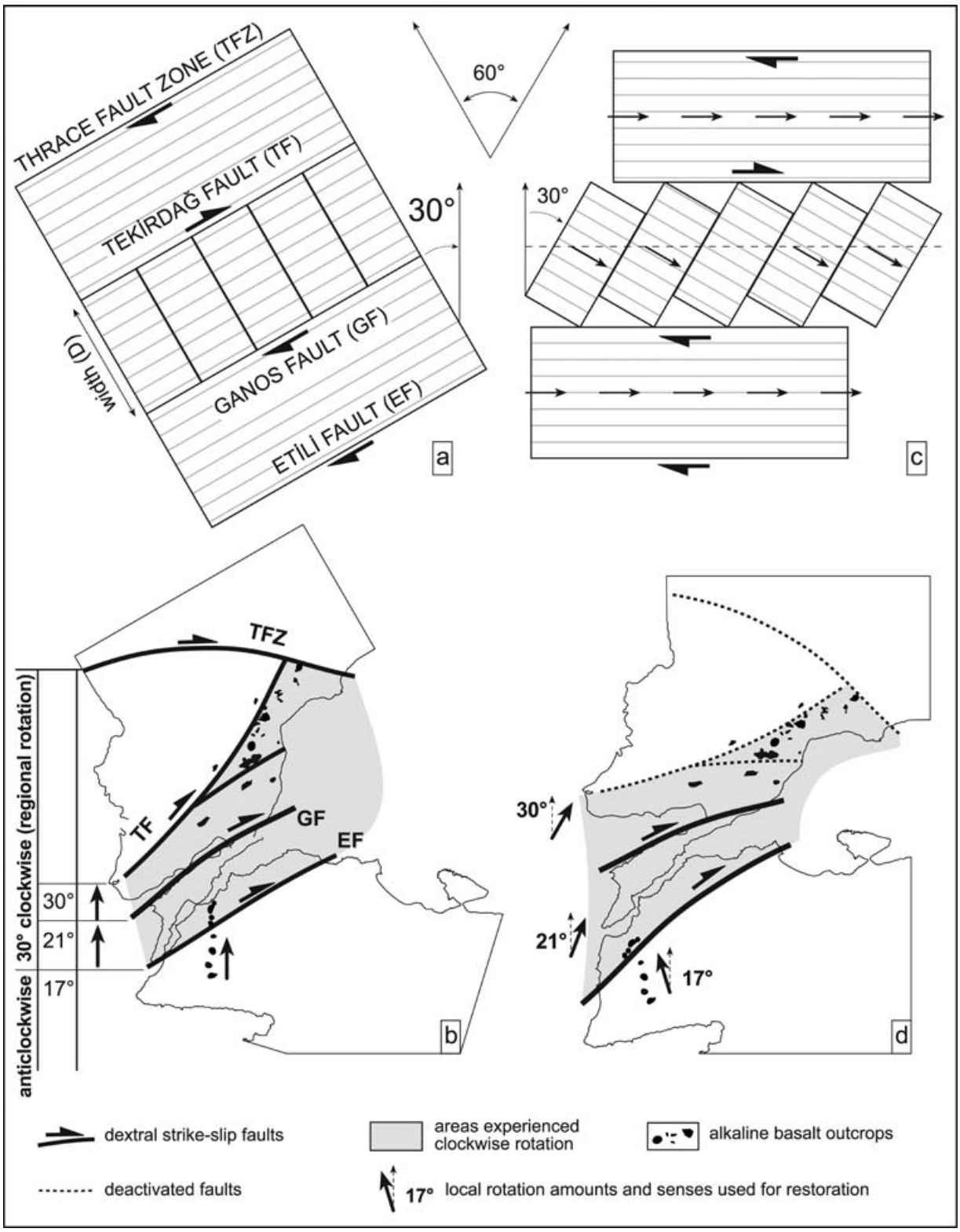

Figure 7. Tentative models proposed to explain development of clockwise and anticlockwise rotations of the lava flows in NW Turkey. (a) schematized and (b) simplified restored configuration of the NW Anatolia, (c) schematized and (d) simplified present configuration of the region. Note that after the restoration the basalt outcrops are aligned N–S. Note also that 60° clockwise rotation of the area between the Tekirdağ and Ganos faults resulted from 30° regional and further 30° local rotation of the area.

pre-existing structures, some of which were reactivated by the North Anatolian Fault Zone during Pleistocene times (see also Yaltırak & Alpar, 2002), or the inception age of the North Anatolian Fault Zone is at least Late Miocene or older as proposed by Zattin, Okay & Cavazza (2005).

7. Concluding remarks

Northwestern Turkey contains a number of intra-continental alkaline volcanic eruptive sequences formed along the localized shear zones bounded by sub-parallel dextral strike-slip faults. Eruption of basaltic lavas occurred synchronously both in the Thrace basin (8.43 ± 0.07 to 11.68 ± 0.25 Ma) and in the Biga Peninsula (7.65 ± 0.36 to 11.16 ± 0.21 Ma), indicating an approximately 4 million year episode of volcanic activity for the whole area. Palaeomagnetic measurements from these two regions, however, indicate that the lavas in the Thrace basin were rotated clockwise by up to 73° and that they are constrained within a shear zone delimited by the Tekirdağ Fault in the north and Ganos Fault in the south, while those in the Biga Peninsula were mostly rotated clockwise by up to 33° with rotation attributed to movements along the Edremit, Yenice and Etili faults. Potential models to account for rotations in the region include: (1) large regional rotations slightly modified by local rotations and (2) block rotations within dextral shear zones with comparable regional rotation. Based on larger clockwise rotation within the area located between the Tekirdağ and Ganos faults and smaller clockwise rotation outside of this area, the second model is favoured. Overall, our palaeomagnetic and ^{40}Ar–^{39}Ar data suggest that NW Turkey experienced strike-slip activity prior to mid-Pliocene times and during the Late Miocene; this implies that the region experienced dextral strike-slip activity prior to the Late Pliocene development of the North Anatolian Fault Zone. This implies that the ENE-trending active faults in the region including the Ganos, Etili, Yenice and Edremit fault zones are pre-existing structures and were subsequently reactivated after the inception of the North Anatolian Fault Zone in Late Pliocene times. Otherwise, the inception age of the North Anatolian Fault Zone is older than it is thought to be and must be as old as Late Miocene, and hence the North Anatolian Fault Zone controlled the eruption of the alkaline basalts in the region.

Acknowledgements. We thank Hayfaa Abdulaziz, for her help in sample preparation and interpretation of the results in the Fort hoofddijk Laboratory. Pınar Ertepınar helped with measuring the samples. Bas Steins and Şenol Özmutlu supplied accommodation in the Netherlands. This research was funded by TUBITAK grant YDABAG-102Y069 and partly by the Middle East Basins Evolution project no: 16–02 (MEBE, CNRS-France). We are grateful to John Piper and Chris Rowan for their constructive review and helpful suggestions.

References

ALDANMAZ, E. 2002. Mantle source characteristics of alkali basalts and basanites in an extensional intra-continental plate setting, western Anatolia, Turkey: Implication for multi-stage melting. *International Geology Review* **44**, 440–57.

ALDANMAZ, E, GOURGAUD, A. & KAYMAKCI, N. 2005. Constraints on the composition and thermal structure of the upper mantle beneath NW Turkey: evidence from mantle xenoliths and alkali primary melts. *Journal of Geodynamics* **39**, 277–316.

ALDANMAZ, E., KOPRUBASI, N., GURER, O. F., KAYMAKCI, N. & GOURGAUD, A. 2006. Geochemical constraints on the Cenozoic, OIB-type alkaline volcanic rocks of NW Turkey: Implications for mantle sources and melting processes. *Lithos* **86**, 50–76.

ALDANMAZ, E., PEARCE, J. A., THIRLWALL, M. F. & MITCHELL, J. G. 2000. Petrogenetic Evolution of Late Cenozoic, Post-Collision Volcanism in Western Anatolia, Turkey. *Journal of Volcanology and Geothermal Research* **102**, 67–95.

BARKA, A. A. 1992. The North Anatolian fault zone. *Annales Tectonicae* **VI** supp., 164–95.

BARKA, A. A. & HANCOCK, P. L. 1984. Neotectonic deformation patterns in the convex-northwards arc of the North Anatolian Fault Zone. In *The geological evolution of the Eastern Mediterranean* (eds J. E. Dixon & A. H. F. Robertson), pp. 763–74. Geological Society of London, Special Publication no. 17.

BIDDLE, K. T. & CHRISTIE-BLICK, N. 1985. Deformation and basin formation along strike-slip faults. In *Strike-slip deformation, basin formation and sedimentation* (eds K. T. Biddle & N. Christie-Blick), pp. 1–45. Society of Economic Palaeontologists and Mineralogistsm Special Publication no. 37.

BOZKURT, E. 2001. Neotectonics of Turkey – a synthesis. *Geodinamica Acta* **14**, 3–30.

COŞKUN, B. 1997. Oil and gas fields – transfer zone relationships, Thrace Basin, NW Turkey. *Marine and Petroleum Geology* **14**, 401–16.

COŞKUN, B. 2000. North Anatolian Fault-Saros Gulf relationships and their relevance to hydrocarbon exploration, northern Aegean Sea, Turkey. *Marine and Petroleum Geology* **17**, 751–72.

DEWEY, J. F., HEMPTON, M. R., KIDD, W. S. F., ŞAROĞLU, F. & ŞENGÖR, A. M. C. 1986. Shortening of continental lithosphere. The neotectonics of eastern Anatolia. In *Collision tectonics* (eds M. P. Coward & A. C. Ries), pp. 3–36. Geological Society of London, Special Publication no. 19.

DIMITRIADIS, S., KONDOPOULOU, D. & ATZEMOGLOU, A. 1998. Dextral rotations and tectonomagmatic evolution of the southern Rhodope and adjacent regions (Greece). *Tectonophysics* **299**, 159–73.

DRESEN, G. 1992. Stress distribution and the orientation of Riedel shears. *Tectonophysics* **188**, 239–47.

DUERMEIJER, C. E., KRIJGSMAN, W., LANGEREIS, C. G., MEULENKAMP, J. E., TRIANTAPHYLLOU, M. V. & ZACHARIASSE, W. J. 1999. A late Pleistocene clockwise rotation phase of Zakynthos (Greece) and implications for the evolution of the western Aegean arc. *Earth and Planetary Science Letters* **173**, 315–31.

DUERMEIJER, C. E., NYST, M., MEIJER, P. TH., LANGEREIS, C. G. & SPAKMAN, W. 2000. Neogene evolution of the Aegean arc: palaeomagnetic and geodetic evidence for a rapid and young rotation phase. *Earth and Planetary Science Letters* **176**, 509–25.

ERCAN, T., SATIR, M., STEINITZ, G., DORA, A., SARIFAKIOGLU, E., ADIS, C., WALTER, H. J. & YILDIRIM, T. 1995. Biga yarımadası ile Gökçeada, Bozcaada ve Tavşan adalarındaki (KB Anadolu Tersiyer volkanizmasının özellikleri (Characteristics of the Tertiary

volcanism in the Biga Peninsula, Gökçeada, Bozcaada and Tavşanadası, NW Anatolia). *Bulletin of Geological Society of Turkey* **28**, 121–36.

EYIDOĞAN, H. 1988. Rates of crustal deformation in western Turkey as deduced from major earthquakes. *Tectonophysics* **148**, 83–92.

FISHER, R. A. 1953. Dispersion on a sphere. *Proceedings of the Royal Society London* **A2/I7**, 295–305.

FLERIT, F., ARMIJO, R., KING, G. & MEYER, B. 2004. The mechanical interaction between the propagating North Anatolian Fault and the back-arc extension in the Aegean. *Earth and Planetary Science Letters* **224**, 347–62.

GANS, P. B. 1997. Large-magnitute Oligo-Miocene extension in southern Sonora: Implications for the tectonic evolution of northwest Mexico. *Tectonics* **16**, 388–408.

GARFUNKEL, Z. 1989. Regional deformation by block translation and rotation. In *Palaeomagnetic Rotations and Continental Deformation* (eds C. Kissel & C. Laj), pp. 181–203. NATO AS1 Series 254.

GÖRÜR, N. & OKAY, A. İ. 1996. A fore-arc origin for the Thrace Basin, NW Turkey. *Geologische Rundschau* **85**, 662–8.

GÜRER, O. F., KAYMAKCI, N., ÇAKIR, S. & ÖZBURAN, M. 2003. Neotectonics of Southeast Marmara Region (NW Anatolia, Turkey). *Journal of Asian Earth Science* **21**, 1041–51.

GÜRSOY, H., PIPER, J. D. A. & TATAR, O. 2003. Neotectonic deformation in the western sector of tectonic escape in Anatolia: palaeomagnetic study of the Afyon region, central Turkey. *Tectonophysics* **374**, 57–79.

GÜRSOY, H., PIPER, J. D. A., TATAR, O. & TEMIZ, H. 1997. A palaeomagnetic study of the Sivas Basin, central Turkey: crustal deformation during lateral extrusion of the Anatolian Block. *Tectonophysics* **271**, 89–105.

KAYMAKCI, N., DUERMEIJER, C. E., LANGEREIS, C., WHITE, S. H. & VANDIJK, P. M. 2003. Palaeomagnetic evolution of the Çankırı Basin (central Anatolia, Turkey): implications for oroclinal bending due to indentation. *Geological Magazine* **140**, 343–55.

KAYMAKCI, N., WHITE, S. H. & VAN DIJK, P. M. 2003. Kinematic and structural development of the Çankiri Basin (Central Anatolia, Turkey): a palaeostress inversion study. *Tectonophysics* **364**, 85–113.

KISSEL, C. & LAJ, C. 1988. The Tertiary geodynamic evolution of the Aegean Arc: a palaeomagnetic reconstruction. *Tectonophysics* **146**, 183–201.

KISSEL, C., LAJ, C., POISSON, A. & GÖRÜR, N. 2003. Palaeomagnetic reconstruction of the Cenozoic evolution of the Eastern Mediterranean *Tectonophysics* **362**, 199–217.

KOÇYIĞIT, A. 1989. Suşehri basin: an active fault-wedge basin on the North Anatolian Fault Zone, Turkey. *Tectonophysics* **167**, 13–29.

KOTZEV, V., NAKOV, R., BURCHFIELD, B. C., KING, R. & REILINGER, R. 2001. GPS study of active tectonics in Bulgaria: results from 1996 to 1998. *Journal of Geodynamics* **31**, 189–200.

MANKINEN, E. & DALRYMPLE, G. 1972. Electron microprobe evaluation of terrestrial basalts for whole-rock K–Ar dating, *Earth Planetary Science Letters* **17**, 89–94.

MCCLUSKY, S., BALASSANIAN, S., BARKA, A. A., DEMIR, C., ERGINTAV, S., GEORGIEV, L., GÜRKAN, O., HAMBURGER, M., HURST, K., KAHLE, H. G., KASTENS, K., KEKELIDZE, G., KING, R., KOTZEV, V., LENK, O., MAHMOUD, S., MISHIN, A., NADARIYA, M., OUZOUNIS, A., PARADISSIS, D., PETER, Y., PRILEPIN, M., REILINGER, R.E., SANLI, I., SEEGER, H., TEALEB, A., TOKSÖZ, M. N. & VEIS, G. 2000. Global Positioning System constraints on plate kinematics and dynamics in the Eastern Mediterranean and Caucasus. *Journal of Geophysical Research* **105**, 5695–720.

MCKENZIE, D. 1972. Active tectonics of the Mediterranean region. *Geophysical Journal of the Royal Astronomical Society* **30**, 109–85.

OKAY, A. I., KAŞLILAR-ÖZCAN, A., İMREN, C., BOZTEPE-GÜNEY, A., DEMIRBAĞ, E. & KUŞÇU, I. 2000. Active faults and evolving strike-slip basins in the Marmara Sea, northwest Turkey: a multichannel seismic reflection study. *Tectonophysics* **321**, 189–218.

OKAY, A. I., TÜYSÜZ, O. & KAYA, Ş. 2004. From transpression to transtension: changes in morphology and structure around a bend on the North Anatolian Fault in the Marmara region. *Tectonophysics* **391**, 259–82.

ORAL, M. B., REILINGER, R. E., TOKSOZ, M. N., KING, R. W., BARKA, A. A., KINIK, I. & LENK, O. 1995. Global positioning system offers evidence of plate motions in Eastern Mediterranean. *EOS, Transactions American Geophysical Union* **76**, 9–11.

PERINÇEK, D. 1991. Possible strand of the North Anatolian fault in the Thrace Basin, Turkey: an interpretation. *American Association of Petroleum Geologists Bulletin* **75**, 241–57.

PIPER, J. D. A., GÜRSOY, H. & TATAR, O. 2002. Palaeomagnetism and magnetic properties of the Cappadocian ignimbrite succession, central Turkey and Neogene tectonics of the Anatolian collage. *Journal of Volcanology and Geothermal Research* **117**, 237–62.

PIPER, J. D. A., MOORE, J., TATAR, O., GÜRSOY, H. & PARK, R. G. 1996. Palaeomagnetic study of crustal deformation across an intracontinental transform: the North Anatolian Fault Zone in Northern Turkey. In *Palaeomagnetism of the Eastern Mediterranean Region* (eds A. Morris & D. H. Tarling), pp. 299–310. Geological Society of London, Special Publication no. 105.

PLATZMAN, E. S., PLATT, J. P., TAPIRDAMAZ, C., SANVER, M. & RUNDLE, C. C. 1994. Why are there no clockwise rotations along the North Anatolian Fault? *Journal of Geophysical Research* **99**, 21705–16.

PLATZMAN, E. S., TAPIRDAMAZ, C. & SANVER, M. 1998. Neogene anticlockwise rotation of central Anatolia (Turkey): Preliminary palaeomagnetic and geochronological results. *Tectonophysics* **299**, 175–89.

PROVOST, A. S., CHÉRY, J. & HASSANI, R. 2003. 3D mechanical modeling of the GPS velocity field along the North Anatolian fault. *Earth and Planetary Science Letters* **209**, 361–77.

REILINGER, R. E., MCCLUSKY, S. C., ORAL, M. B., KING, W. & TOKSÖZ, M. N. 1997. Global Positioning System measurements of present-day crustal movements in the Arabian-Africa-Eurasia plate collision zone, *Journal of Geophysical Research* **102**, 9983–99.

RON, H., FREUND, R., GARFUNKEL, Z. & NUR, A. 1984. Block rotation by strike slip faulting: structural and palaeomagnetic evidence. *Journal of Geophysical Research* **89**, 6256–70.

ROTSTEIN, Y. 1984. Counterclockwise rotation of the Anatolian block. *Tectonophysics* **108**, 71–91.

SAKINÇ, M., YALTIRAK, C. & OKTAY, F. Y. 1999. Palaeogeographical evolution of the Thrace Neogene Basin and the Tethys–Paratethys relations at northwestern

Turkey (Thrace). *Palaeogeography, Palaeoclimatology, Palaeoecology* **153**, 17–40.

SATO, T., KASAHARA, J., TAYMAZ, T., ITO, M., KAMIMURA, A., HAYAKAWA, T. & TAN, O. 2004. A study of microearthquake seismicity and focal mechanisms within the Sea of Marmara (NW Turkey) using ocean bottom seismometers (OBSs). *Tectonophysics* **391**, 300–14.

ŞAROĞLU, F. 1988. Age and off-set of the North Anatolian Fault. *METU, Journal of Pure and Applied Sciences* **21**, 65–79.

ŞENGÖR, A. M. C., GÖRÜR, N. & ŞAROĞLU, F. 1985. Strike-slip deformation and related basin formation in zones of tectonic escape: Turkey as acase study. In *Strike-slip deformation, basin formation and sedimentation* (eds K. T. Biddle & N. Christie-Blick), pp. 227–64. *Society of Economic Palaeontologists and Mineralogists*, Special Publication no. 37.

SIYAKO, M., BÜRKAN, K. A. & OKAY, A. I. 1992. Tertiary geology and hydrocarbon potential of the Biga and Gelibolu peninsulas. *Bulletin Turkish Association of Petroleum Geologists* **1**, 183–99 (in Turkish).

SPELL, T. L. & MCDOUGALL, I. 2003. Characterization and calibration of $^{40}Ar/^{39}Ar$ dating. Standards. *Chemical Geology* **198**, 189–211.

STAUDACHER, T. H., JESSBERGER, E. K., DORFLINGER, D. & KIKO, J. 1978. A refined ultrahigh-vacuum furnace for rare gas analysis. *Journal of Physics Series E: Scientific Instruments* **11**, 781–4.

SYLVESTER, A. G. 1988. Strike-slip faults. *Bulletin of Geological Society of America* **100**, 1666–1703.

TAPIRDAMAZ, C. & YALTIRAK, C. 1997. Trakya'da Senozoyik volkaniklerinin palaeomanyetik özellikleri ve bölgenin tektonik evrimi. *Maden Tetkik ve Arama Enstitüsü Bülteni* **119**, 27–42.

TATAR, O., PIPER, J. D. A., PARK, R. G. & GÜRSOY, H. 1995. Palaeomagnetic study of block rotations in the Niksar overlap region of the North Anatolian Fault Zone, Central Turkey. *Tectonophysics* **244**, 251–66.

TATAR, O., PIPER, J. D. A., GÜRSOY, H., HEIMANN, A. & KOÇBULUT, F. 2004. Neotectonic deformation in the transition zone between the Dead Sea Transform and the East Anatolian Fault Zone, Southern Turkey: a palaeomagnetic study of the Karasu Rift Volcanism. *Tectonophysics* **385**, 17–43.

TURGUT, S., TÜRKASLAN, M. & PERINÇEK, D. 1991. Evolution of the Thrace sedimentary basin and hydrocarbon prospectivity. In *Generation, Accumulation and Production of Europe's Hydrocarbon* (ed. A. M. Spencer), pp. 415–37. European Association of Petroleum Geosciences, Special Publication no. 1.

TÜYSÜZ, O., BARKA, A. & YIĞITBAŞ, E. 1998. Geology of the Saros graben and its implications for the evolution of the North Anatolian fault in the Ganos–Saros region, northwestern Turkey. *Tectonophysics* **293**, 105–26.

TWISS, R. J. & MOORES, E. M. 1992. *Structural Geology.* New York: Freeman and Co.

VAN HINSBERGEN, D. J. J. 2004. The evolving anatomy of a collapsing orogen. Published Ph.D. thesis, Utrecht University, The Netherlands, 280 pp. *Geologica Ultraiectina* **243**.

YALTIRAK, C. 1996. Tectonic history of the Ganos fault system (in Turkish with English abstract). *Bulletin of Turkish Association of Petroleum Geologists* **8**, 137–56.

YALTIRAK, C. 2002. Tectonic evolution of the Marmara Sea and its surroundings. *Marine Geology* **190**, 367–82.

YALTIRAK, C. & ALPAR, B. 2002. Kinematics and evolution of the northern branch of the North Anatolian Fault (Ganos Fault) between the Sea of Marmara and the Gulf of Saros. *Marine Geology* **190**, 351–66.

YILMAZ, Y. & KARACIK, Z. 2001. Geology of the northern side of the Gulf of Edremit and its tectonic significance for the development of the Aegean grabens. *Geodinamica Acta* **14**, 31–43.

YILMAZ, Y. & POLAT, A. 1998. Geology and evolution of the Thrace volcanism, Turkey. *Acta Vulcanologica* **10**, 293–303.

ZATTIN, M., OKAY, A. I. & CAVAZZA, W. 2005. Fission-track evidence for late Oligocene and mid-Miocene activity along the North Anatolian Fault in southwestern Thrace. *Terra Nova* **17**, 95–101.

ZIJDERVELD, J. D. A. 1967. Demagnetisation of rock: analysis of results. In *Methods in palaeomagnetism* (eds D. W. Collinson, K. M. Creer & S. K. Runcorn), pp. 254–86. Amsterdam: Elsevier.